2023 IEEE International Conference on Robotics and Automation (ICRA 2023)
May 29 - June 2, 2023. London, UK

Rendezvous and Docking of Magnetic Helical Microrobots Along Arc Orbits for Field-directed Assembly and Disassembly*

Shuideng Wang, *Student Member, IEEE,* Zejie Yu, *Student Member, IEEE,* Chaojian Hou, *Student Member, IEEE,* Kun Wang, *Student Member, IEEE,* and Lixin Dong, *Senior Member, IEEE*

***Abstract*—Due to the limited cargo/functional element loading and other capabilities of individual microrobots, assembling them for locomotion and disassembling them as arriving at the target is more effective. An approach called rendezvous and docking is proposed in this paper to control the assembly and disassembly of helical microrobots actuated by a uniform rotating magnetic field. Docking is realized around the intersection of their arc orbits with the assistance of a fluidic field. To adjust the distance between the adjacent helical robots suspending in solution but with a distance beyond the acceptable range of the magnetic interaction, their asynchronized velocities are achieved using the interaction between the robots and fluids. For robots rotating at different speeds around their longitudinal axes at a driving frequency lower than the cut-off frequency, different fluidic flows will be generated. Based on the interaction between the robots and the fluids, the translational trajectory paths may be tuned, causing the adjacent robots to move closer. Docking along the tangential direction of rendezvous arc trajectories avoids the instability of the helical robot rotating around the radial direction and the problem of excessive linear speed at the end during assembly so that the robot can rotate stably around its axis while completing the assembly. Besides these, assembled microrobots can also lower the requirements on the imaging resolution of motion tracking and the forces for driving; hence much lower cost for both imaging and driving equipment.**

I. Introduction

Magnetically driven microrobots have promising application prospects in the field of biomedicine because of their small sizes and the low magnetic induction intensity of the magnetic field driving them [1-4]. The small scale of a microrobot determines that its output and carrying capacity are minimal. Therefore, assembly and disassembly are effective means when facing objects more considerable than the size of the microrobot. So far, a few works on self-assembly have been demonstrated on various types of robots, such as colloids [5, 6], nano-cubes [7], magnetic microspheres [8, 9], and even peanut-like shapes [10]. However, these are assembled by local magnetic induction and magnetic interaction. Local magnetic induction has a limited effective distance, whereas the gradient magnetic field is not always available or applicable. Furthermore, the field with a gradient could actuate a complex motion with some particular field gradient distribution. However, the robots will still follow the direction that makes their magnetic potential decrease fastest. In other words, robots actuated by a gradient field are more like a one-dimension motion. In contrast, a robot with a helical structure can naturally use the interaction with the fluid to convert rotary power provided by the field to linear translation [11-13], not to mention that a low-strength field can actuate it.

Magnetic helical robots have developed rapidly in the past decade because of the advantage of this expansion of motion functions [14]. Some helical robots with heads actuate the body, transporting cargo, or other functions [12, 15, 16], while others are made entirely of helix [17, 18]. Among them, new assemblies composed of purely helical robots have significantly better homogeneity and scalability, which is beneficial for self-assembly with massive amounts.

However, the relatively complex structure of the helix, while bringing more possibilities for motion, also poses a problem for self-assembly. The most challenging problem is that the radial moment of inertia is too large. The helix is a typical structure with axial and radial differences, and the ratio of the moment of inertia in the two directions is inversely proportional to the square of the ratio of its scale. So, the helical swimmer suspended in the solution constantly rotates around the axis direction spontaneously. Though a single helical robot can rotate around the radial direction with the support of the substrate, the assembly will fail to do this. Because it will always become longer and longer as the assembly progresses, and the radial moment of inertia increases with the square of the length. Therefore, this paper proposes a method to allow the helix to assemble around arc orbits while maintaining its axial rotation. Related disassembly methods are also considered.

II. Rendezvous and Docking

A. Magnetic Moment of Robots

Because the local magnetic interaction is chosen as the connecting force for assembly, the global and local magnetic moments of the robot must be carefully designed. Therefore, we adopted the silicon nitride helix fabricated by the self-scrolling method [19] and uniformly deposited a nickel layer on it as a magnetic material. Considering that the limit diameter D_{sp} of the superparamagnetic material of nickel is about 32 nm [20], we set the film thickness to 65 nm to ensure that any part of the robot can retain a certain remanence after being magnetized from any direction. For magnetic materials whose dimensions are more significant than the single domain limit, the direction of the easy axis will be along the longest

*This work was partially supported by the National Natural Science Foundation of China (grant no. 62127810) and the General Research Fund of Hong Kong (Project nos. 11219419, 11213720, and 11217221).

All authors are with the Department of Biomedical Engineering, City University of Hong Kong, Hong Kong, 999077, China (email: Stone.wang@my.cityu.edu.hk; zejieyu2-c@my.cityu.edu.hk; chaojhou@cityu.edu.hk; k.wang@my.cityu.edu.hk; corresponding author to provide phone: +852-3442-9545; email: l.x.dong@cityu.edu.hk).

axis of the entire material, which can be verified by the approximate calculation equation of the demagnetization factor of the cylinder:

$$N_l = \frac{1}{k^2-1}\left(\frac{k}{2\sqrt{k^2-1}}\ln\frac{k+\sqrt{k^2-1}}{k-\sqrt{k^2-1}}-1\right) \quad (1)$$

where k is the cylinder aspect ratio, N_l is the longitudinal direction factor, and there is a radial direction factor N_d, which meets the equation $N_l + 2N_d = 1$. With the nickel film having a length of 200 μm, a width of 20 μm, and a thickness of 65 nm, the demagnetization factor difference of the diagonal direction δN is about 0.48. That verified that the easy axis is along the diagonal direction shown in Fig. 1(a). After scrolling, the line where the easy axis is located will form the spiral line in Fig. 1(b). In order to simplify the consideration of magnetization, the helix is divided into eight regions in the circumferential direction, and the easy axis direction of each region is shown in Fig. 1 (c).

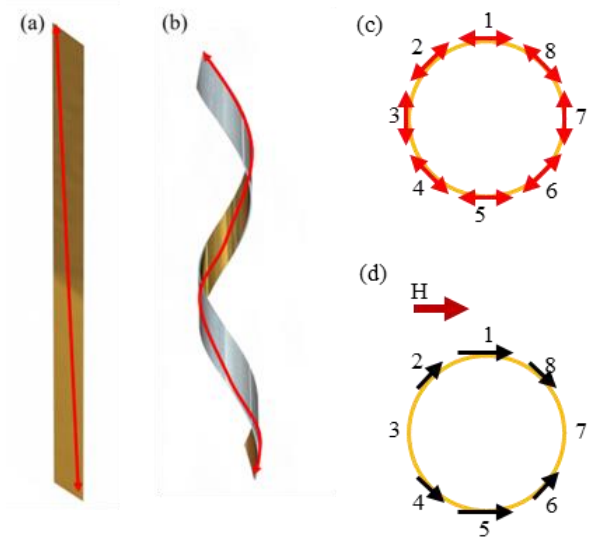

Figure 1. Easy axes of the helical robot: (a) before and (b) after self-scrolling, (c) the easy axis direction of eight regions after the helical robot self-scrolling, (d) schematic diagram of the magnitude and direction of residual magnetism in each region after applying and removing a magnetizing magnetic field.

Considering the rotary feed motion of the helical robot, its total magnetic moment should be along the radial direction of the helix, so the direction of the external magnetic field used for magnetization is also along the radial direction. For each region, the larger the angle between the direction of the magnetizing magnetic field and its easy axis, the smaller the remanence after removing the magnetic field. Therefore, after magnetization, the projection of the magnetic moment distributed on the helical robot on the circumferential plane should be shown in Fig. 1(d). In the case of this kind of magnetic moment distribution, if the helix has an integer pitch, its head and tail will generally be in the No. 7 or No. 3 area in Fig. 1(d), so that the magnetic interaction cannot be well utilized when docking. Therefore, a helix with slightly less than integer turns should be chosen to get a more significant magnetic moment at the head and tail.

B. *Fluid Interactions*

Given that the motion of the helical robot is to rotate while translating in the direction of the axis, it would be insufficient only to consider its forward motion guided by the magnetic field by ignoring the interaction of fluids driven by rotating robots, which will also influence the adjacent robots. For a rotating bulk robot, whether it is laminar flow at a low Reynolds number or turbulent flow at a slightly higher Reynolds number, it can be calculated or simulated [21, 22], which can provide approximate estimates for the fluid movement around the helical robot with a more complex structure.

The first thing to consider is whether the fluid around the helical robot is laminar or turbulent. After a simple deformation of the Reynolds number equation $\mathrm{Re} = v\rho d/\mu$, we obtained:

$$\mathrm{Re} = \frac{\pi f \rho d^2}{\mu} \quad (2)$$

where f is the rotational frequency of the robot and d is the diameter of the robot. With the diameter of 16 μm and the liquid density and viscosity the same as water, when the rotation frequency is 1, the Reynolds number is about 0.008. However, it is difficult to determine if it is sufficiently low. In order to make the robot run at a low enough Reynolds number, the viscosity of the liquid is increased in our experiment to ensure that the fluid around the robot is in a laminar flow state. At this time, the fluid velocity is proportional to the rotational speed of the robot according to the viscosity law.

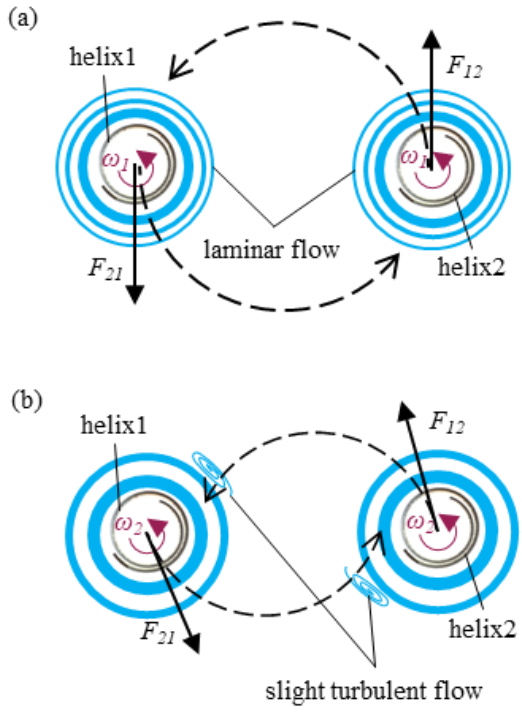

Figure 2. Scheme of binary star system (a) at low *Re* and (b) a little higher than low *Re*, F_{12} represents the force of helix 2 on helix 1, and F_{21} is similar.

For adjacent helical robots at a fixed distance x, when their angular velocity around their axis direction is low, the force exerted by the laminar fluid on distance x is not enough to affect each other. Therefore the positions of the two robots remain relatively static. On the other hand, when the velocity increases, the fluid around the robots will give each other a force perpendicular to the line between the two robots, causing the two robots to "revolve" around the midpoint of the line while rotating around their axes; thus a bi-star system is formed (Fig. 2(a)).

However, when the angular velocity of the robot is further increased, it will not fully meet the low Reynolds number condition. At this time, the slight turbulence around the robot will disturb the stability of the binary system and make the two robots gradually approach (Fig. 2(b)), which can be used to adjust the distance between the two robots.

C. *Assembly and Disassembly*

Adjusting the distance between the two helical robots not limited to the method mentioned above can be made close to one body length. In this case, the easiest way to assemble is to rotate the robot around its radial direction. However, due to the difference in rotational inertia, the helical robot freely suspended in the solution will spontaneously revolve around the direction of more negligible rotational inertia, the axis direction. Therefore, it is best to keep the two robots in their forward direction at this time and make them close end to end by detouring an arc trajectory no more than $\pi/2$.

As shown in Fig. 3(a), the two helical robots with the head aligned swim around a quarter of a circle to get assembled. Nevertheless, the strategy of two robots with heads not aligned (Fig. 3(b)) should be briefly calculated first.

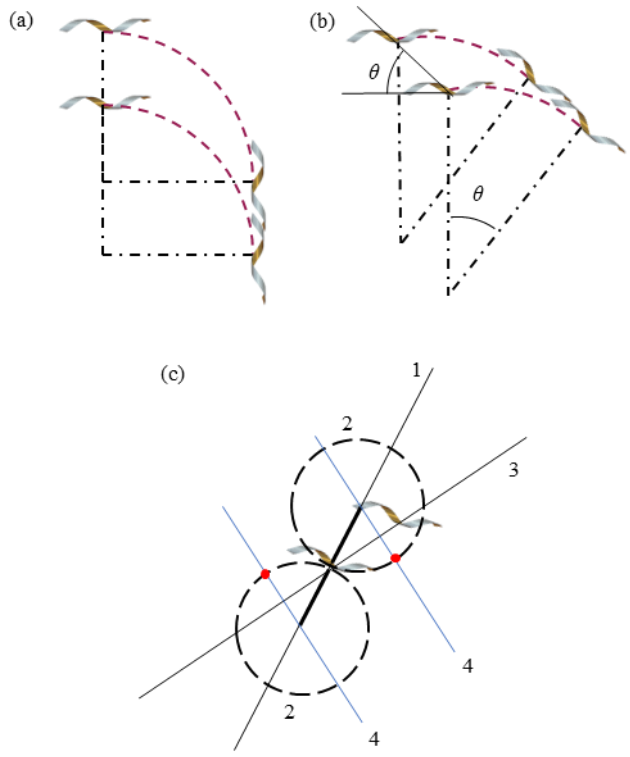

Figure 3. Rendezvous and docking: Two robots at a distance of one body length with their heads (a) aligned and (b) not aligned are assembled after swimming along an arc orbit. (c) the strategy scheme of two robots with heads not aligned, in which the numbers represent the solving step order.

Due to the synchronization of the two helical robots, only one of the arc trajectories needs to be calculated, and the other trajectory can be obtained by translating the calculated trajectory by one body length along the line connecting the centroids of the two robots. As shown in Fig. 3(c), the solution of the strategy has four steps:

- Choose a helix and draw a straight-line l perpendicular to its axis through its center of mass. The center of the trajectory must be on this line l.
- Since the angular velocity of the yaw is relatively independent of the angular velocity of the yaw around itself when the spiral orbits the trajectory, the radius of the arc trajectory can be adjusted. If a radius R is selected, the point on the straight-line l with the distance R from the helix is the center of the trajectory at a specific yaw angular velocity.
- Draw a line m that coincides with the line connecting the centroids of the two robots. Again, according to the synchronicity of the two robot motions, it can be concluded that line m is perpendicular to the line connecting the center of the circle at the final intersection point.
- Draw perpendicular lines to the line m through the two centers of the circles, and these two perpendicular lines intersect the circle to obtain four intersection points. These four intersections are all points where assembly can be achieved.

Since the helical robots can choose any axis direction to move forward, two of the points are better because they are closer to the robots, which also proves that the arc of the arc trajectory mentioned above must be no greater than $\pi/2$.

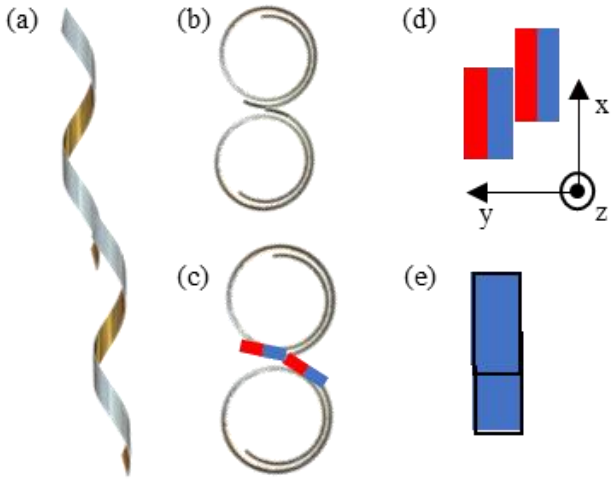

Figure 4. The torque generated by the field: (a) without and (b) with an additional angular velocity perpendicular to the robot axis.

To analyze disassembly, firstly need to determine the state of the magnetic connection between the robots. According to the distribution of the robot's magnetic moment, after the two robots are assembled, they are mostly connected, as shown in Fig. 4(a)-(c). For small magnetic moments that locally constitute magnetic connections, viewing in side view should yield magnetic pairs as shown in Fig. 4(d), Fig. 4(e), or at some angle in between them. Pulling in the axial direction requires the most effort to separate a pair of magnets attached. Due to the large angular velocity of the robot rotating around the axial direction, the changes in the y and z directions of the robot are persistent. If a force is applied in one of these two directions, it is easy to encounter a situation where work is done in the direction of the magnetic interaction, causing the disassembly to fail. The x-direction is a perfect direction, but for robots swimming in low Reynolds numbers, the propulsion matrices of two robots with the same characteristic shape can be linearly superimposed [23], resulting in a more powerful propulsion matrix. So, it is difficult to generate the desired disassembly force in the direction in which the spiral is advancing.

Considering the use of torque, the torque around the x-axis coincides with the direction of the torque generated by the magnetic field driving the robot, and it is still difficult to achieve a higher cut-off frequency. However, around the y and z directions, the solution assembly is easy to achieve. Taking a moment around the z-axis as an example, for the case of Fig. 4(d), there is no complete work against the magnetic force. In the case of Fig. 4(e), it is entirely perpendicular to the direction of the magnetic interaction. Therefore, a relatively large torque needs to be applied in the direction perpendicular to the axial direction of the helical robot to complete the disassembly.

The specific implementation method is to make the magnetic field apply a large rate of angular change in the direction perpendicular to the robot axis so that at any instant, the magnetic induction intensity will additionally lead the total magnetic moment of the robot by a large angle, generating a larger moment according to the equation $T = m \times \mu_0 H$. In the process of conducting this moment inside the connecting body, a trend of separating two local magnetic moments is formed. Because this trend does not complete in the opposite direction of the magnetic interaction, the required work will be relatively less, thus easier to disassemble.

The selected robot is a 1.75-turn (pitch) helical robot, as shown in Fig. 5(a), and the magnetic field controlling its motion is a rotating magnetic field based on the homogeneous induction intensity of a three-dimensional electromagnetic Helmholtz coil (Fig. 5(b)). At the same time, to ensure that the robot is in the low Reynolds number range when applying most rotation frequencies, a 70% glycerin solution was injected into the swimming pool to increase the fluid viscosity to 22.5 mPas (the experimental environment temperature was 20 °C).

III. Experimental Results

A. Bi-star Systems

In order to verify the method of adjusting the distance between helical robots with the double-star orbit, the main experiment uses two couples of helical robots with different distances x_1 and x_2 ($x_1 \geqslant x_2$). Apply a high-frequency rotating field to the pair of helixes with a distance of x_1 while applying a low-frequency rotating field to those with a distance of x_2.

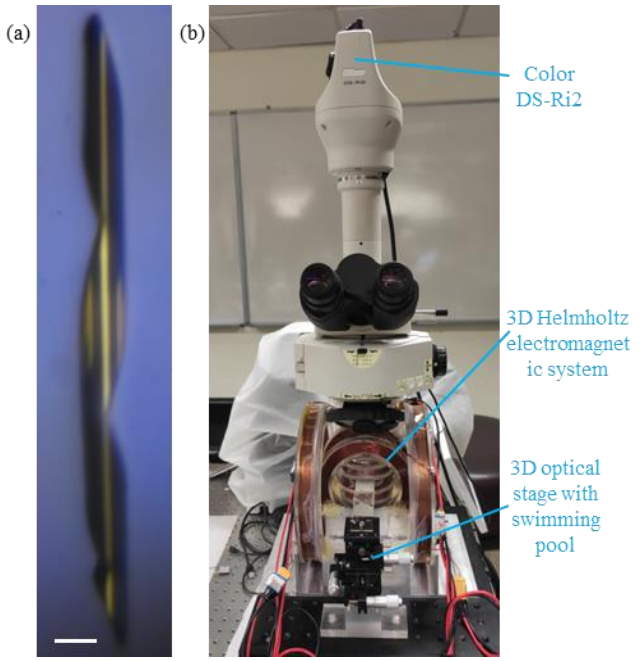

Figure 5. (a) The helical robot (scale bar is 20 μm) and (b) the electromagnetic control system used in the experiment.

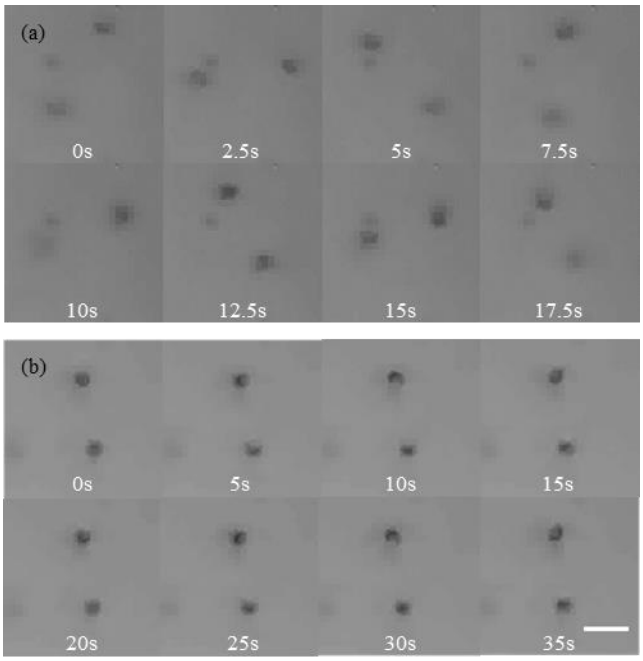

Figure 6. Image sequences of helical robots (a) circle and approach each other and (b) stay in situ (scale bar is 50 μm).

A uniform magnetic field with a magnetic induction of 8 mT was applied to both high (10 Hz) and low (0.1 Hz) frequency situations. The robots circle and slowly approach each other under the high-frequency field and stay in situ under the low-frequency field. Comparing the time of 0 s in Fig. 6(a) and (b), it is clearly shown that the initial distance

between the two robots at low frequency is smaller than that at high frequency. Besides, Fig. 6(b) also shows that the two robots do not approach each other at a low driving frequency, indicating that the mutual attraction of the binary star system is not due to magnetic interaction.

B. Assembly Around an Arc Orbit and Disassembly

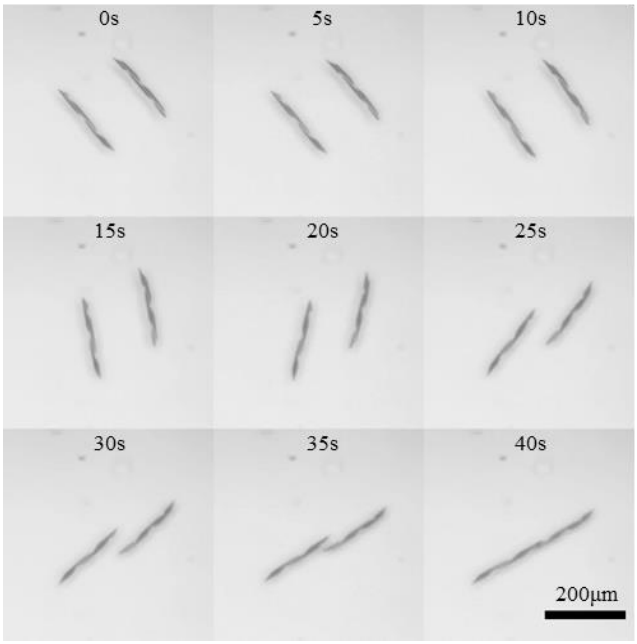

Figure 7. Image sequences of assembly of helical robots along arc orbits.

Fig. 7 shows the assembly of two parallel and head-aligned helical robots around arc trajectories. It passed a quarter arc trajectory before the assembly was finished, with the most prominent arc among all cases of assembly around arc trajectories. By accomplishing this case, the feasibility of assembly along arc orbits was proved.

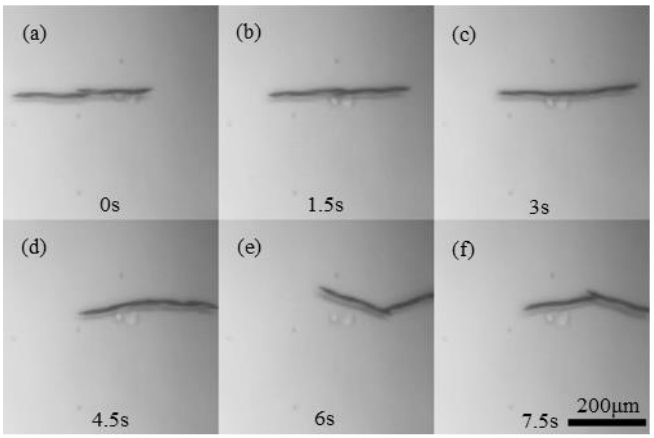

Figure 8. Image sequences of disassembly of helical robots.

The results also demonstrate that the assembly along the orbit can be completed even with a small radius of curvature of the trajectory, keeping the helical robots swimming steadily.

At the time presented by Fig. 8(c) (t = 3s), a large angular velocity, whose value is $\pi/2$ rad/s, with a direction perpendicular to the plane of view, was applied to the magnetic induction. Moreover, in Fig. 8(e) (t = 6s), the assembly is disassembled.

IV. Conclusion

We have shown that rendezvous and docking are effective ways to assemble helical microrobots around arc orbits in a uniform rotating magnetic field with the assistance of a fluidic field. Assembly of microrobots has an enhanced cargo/functional element loading capability. It can boost driving efficiency, hence lowering the requirements on the imaging resolution of motion tracking and the forces for driving.

By applying an angular velocity in an additional direction to the rotating magnetic field, a relatively labor-saving disassembly process partially perpendicular to the direction of the magnetic interaction of the connection point was realized. In addition, the distance adjustment between the two rotating helical robots was realized by using the fine turbulent flow in the operating environment slightly out of the low Reynolds number range, which provided another method for distance adjustment of adjacent robots suspended in liquid with distances greater than the magnetic interaction range. Besides lower costs for imaging and driving equipment, the robustness of assembled microrobots is also higher than swarms.

Acknowledgment

The authors acknowledge the assistance of SUSTech Core Research Facilities.

References

[1] K. E. Peyer, L. Zhang, and B. J. Nelson, "Bio-inspired magnetic swimming microrobots for biomedical applications," *Nanoscale,* vol. 5, no. 4, pp. 1259-1272, 2013.

[2] M. Sitti, H. Ceylan, W. Q. Hu, J. Giltinan, M. Turan, S. Yim, and E. Diller, "Biomedical applications of untethered mobile milli/microrobots," *Proceedings of the IEEE,* vol. 103, no. 2, pp. 205-224, Feb 2015.

[3] D. Loghin, C. Tremblay, M. Mohammadi, and S. Martel, "Exploiting the responses of magnetotactic bacteria robotic agents to enhance displacement control and swarm formation for drug delivery platforms," *International Journal of Robotics Research,* vol. 36, no. 11, pp. 1195-1210, Sep 2017.

[4] Z. Y. Li, C. Y. Li, L. X. Dong, and J. Zhao, "A review of microrobot's system: Towards system integration for autonomous actuation in vivo," *Micromachines,* vol. 12, no. 10, art. no. 1249, Oct 2021.

[5] J. J. Crassous, A. M. Mihut, E. Wernersson, P. Pfleiderer, J. Vermant, P. Linse, and P. Schurtenberger, "Field-induced assembly of colloidal ellipsoids into well-defined microtubules," *Nature Communications,* vol. 5, p. 7, art. no. 5516, Nov 2014.

[6] Q. Chen, S. C. Bae, and S. Granick, "Directed self-assembly of a colloidal kagome lattice," *Nature,* vol. 469, no. 7330, pp. 381-384, Jan 2011.

[7] G. Singh, H. Chan, A. Baskin, E. Gelman, N. Repnin, P. Kral, and R. Klajn, "Self-assembly of magnetite nanocubes into helical superstructures," *Science,* vol. 345, no. 6201, pp. 1149-1153, Sep 2014.

[8] T. T. Xu, Z. M. Hao, J. F. Yu, L. Zhang, X. Y. Wu, and C. Huang, "Multimodal locomotion control of needle-like microrobots assembled by ferromagnetic nanoparticles," *IEEE/ASME Transactions on Mechatronics,* 2022.

[9] B. Yigit, Y. Alapan, and M. Sitti, "Programmable collective behavior in dynamically self-assembled mobile microrobotic swarms," *Advanced Science,* vol. 6, no. 6, art. no. 1801837, Mar 2019.

[10] H. Xie, X. J. Fan, M. M. Sun, Z. H. Lin, Q. He, and L. N. Sun, "Programmable generation and motion control of a snakelike magnetic microrobot swarm," *IEEE/ASME Transactions on Mechatronics,* vol. 24, no. 3, pp. 902-912, Jun 2019.

[11] S. Sudo, S. Segawa, and T. Honda, "Magnetic swimming mechanism in a viscous liquid," *Journal of Intelligent Material Systems and Structures,* vol. 17, no. 8-9, pp. 729-736, Aug-Sep 2006.
[12] L. Zhang, J. J. Abbott, L. X. Dong, B. E. Kratochvil, D. Bell, and B. J. Nelson, "Artificial bacterial flagella: Fabrication and magnetic control," *Applied Physics Letters,* vol. 94, no. 6, art. no. 064107, Feb 2009.
[13] J. J. Abbott, K. E. Peyer, M. C. Lagomarsino, L. Zhang, L. X. Dong, I. K. Kaliakatsos, and B. J. Nelson, "How should microrobots swim?," *International Journal of Robotics Research,* vol. 28, no. 11-12, pp. 1434-1447, Nov-Dec 2009.
[14] Y. Dong, L. Wang, V. Iacovacci, X. P. Wang, L. Zhang, and B. J. Nelson, "Magnetic helical micro-/nanomachines: Recent progress and perspective," *Matter,* vol. 5, no. 1, pp. 77-109, Jan 2022.
[15] S. Tottori, L. Zhang, F. M. Qiu, K. K. Krawczyk, A. Franco-Obregon, and B. J. Nelson, "Magnetic helical micromachines: Fabrication, controlled swimming, and cargo transport," *Advanced Materials,* vol. 24, no. 6, pp. 811-816, Feb 2012.
[16] V. M. Kadiri, C. Bussi, A. W. Holle, K. Son, H. Kwon, G. Schutz, M. G. Gutierrez, and P. Fischer, "Biocompatible magnetic micro- and nanodevices: Fabrication of fept nanopropellers and cell transfection," *Advanced Materials,* vol. 32, no. 25, art. no. 2001114, Jun 2020.
[17] C. Peters, O. Ergeneman, B. J. Nelson, C. Hierold, and Ieee, "Superparamagnetic swimming microrobots with adjusted magnetic anisotropy," in *26th IEEE International Conference on Micro Electro Mechanical Systems (MEMS)*, Taipei, TAIWAN, 2013, pp. 564-567.
[18] F. M. Qiu, S. Fujita, R. Mhanna, L. Zhang, B. R. Simona, and B. J. Nelson, "Magnetic helical microswimmers functionalized with lipoplexes for targeted gene delivery," *Advanced Functional Materials,* vol. 25, no. 11, pp. 1666-1671, Mar 2015.
[19] M. L. Pereira and L. A. Ribeiro, "Self-folding and self-scrolling mechanisms of edge-deformed graphene sheets: A molecular dynamics study," *Physical Chemistry Chemical Physics,* vol. 23, no. 28, pp. 15313-15318, Jul 2021.
[20] D. Jiles, *Introduction to magnetism and magnetic materials*: CRC Press, 2015.
[21] F. Martinez-Pedrero, E. Navarro-Argemi, A. Ortiz-Ambriz, I. Pagonabarraga, and P. Tierno, "Emergent hydrodynamic bound states between magnetically powered micropropellers," *Science Advances,* vol. 4, no. 1, art. no. eaap9379, Jan 2018.
[22] S. Choi, H. Choi, and S. M. Kang, "Characteristics of flow over a rotationally oscillating cylinder at low Reynolds number," *Physics of Fluids,* vol. 14, no. 8, pp. 2767-2777, Aug 2002.
[23] E. M. Purcell, "The efficiency of propulsion by a rotating flagellum," *Proceedings of the National Academy of Sciences of the United States of America,* vol. 94, no. 21, pp. 11307-11311, Oct 1997.